5-2014

Ultra-wideband position tracking on an assembly line

Harikrishnan Ravikrishnan
Clemson University, hra@g.clemson.edu

Ultra-wideband position tracking on an assembly line

A Thesis
Presented to
the Graduate School of
Clemson University

In Partial Fulfillment
of the Requirements for the Degree
Master of Science
Electrical Engineering

---

by
Harikrishnan Ravikrishnan
May 2014

Accepted by:
Dr. Adam W. Hoover, Chair
Dr. Ian D. Walker
Dr. Richard E. Groff

Abstract

This works considers the problem of tracking objects on an assembly line using an ultra-wideband (UWB) positioning system. Assembly line tracking can be accomplished using touch sensors that physically detect when an object reaches a given location. Such tracking requires sensors placed throughout the entire assembly line, and only provides readings at the sensor locations. In contrast, UWB position tracking utilizes a set of sensors surrounding the whole area, enabling continuous position tracking with less infrastructure. Similar tracking can be accomplished using radio frequency identification (RFID) sensing, but this only provides readings when the parts are near RFID readers. The advantage of UWB position tracking is that it can provide sensor readings continuously throughout the entire tracking area. However, UWB position estimates are noisy, typically having an accuracy of 30-100 cm in a room-to-building sized area. This accuracy is sufficient for monitoring which part of an assembly line a part is currently traversing, but is not accurate enough to enable precise tooling or positioning.

In this work, we are using a map of an assembly line to constrain the motion tracking. This is similar to how a road map can be used to constrain position tracking for a GPS sensor. The idea is that the raw sensor measurements are constrained by the a priori known map of motion along the assembly line. We use these constraints and design a particle filter to improve position tracking accuracy.

Acknowledgments

I would like to thank my advisor Dr. Hoover, for helping me throughout my Master's degree. He has spent countless hours discussing ideas, critiquing my writing and encouraging me. His help and lessons on carpentry made the task of building the cart very enjoyable. I would also like to thank the other members of my committee, Dr. Walker, and Dr. Groff for their time spent reviewing this document and providing valuable input. I would like to thank David Moline for helping me set up the laser on the cart and providing me the necessary things for setting up the experiment.

A very special thanks to Jung Phil Kwon for always being there whenever I have been in need. Be it a ride from the airport, buying components, data collection or troubleshooting, the support and help I have got has been invaluable. The time spent discussing ideas, building the cart and collecting data with JP and Mehmet Gungor have been very enjoyable. Without their help, data collection would have been extremely hard.

Last but not the least I would like to thank my parents and my brother. Their constant encouragement, support, belief and confidence in me has kept me going and motivated me to achieve my goals.

Table of Contents

List of Tables

List of Figures

Chapter 1

Introduction

This thesis considers the problem of tracking objects on an assembly line using an ultra-wideband (UWB) positioning system. A UWB positioning system uses a tag placed on the object of interest to transmit UWB pulses to a set of fixed receivers installed around the tracking area. Position estimates are made using trilateration and related techniques from the received signals. The position estimates can be used to continuously monitor the position of parts moving along the assembly line.

Assembly line tracking can be accomplished using touch sensors that physically detect when an object reaches a given location. Figure 1.1 illustrates an assembly line for car manufacturing. Such tracking requires sensors placed throughout the entire assembly line, and only provides readings at the sensor locations. In contrast, UWB position tracking utilizes a set of sensors surrounding the whole area, enabling continuous position tracking with less infrastructure. Similar tracking can be accomplished using radio frequency identification (RFID) sensing, but this only provides readings when the parts are near RFID readers. The advantage of UWB position tracking is that is can provide sensor readings continuously throughout the entire tracking area. However, UWB position estimates are noisy, typically having an accuracy of 30-100

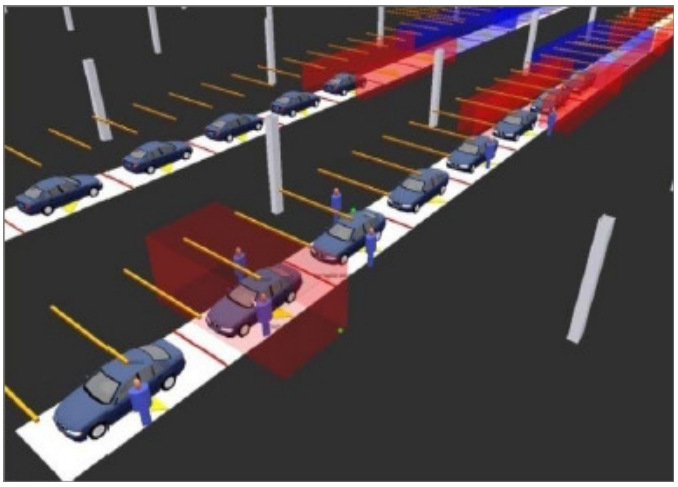

Figure 1.1: Top view of an assembly line for car manufacturing.

cm in a room-to-building sized area [31]. This accuracy is sufficient for monitoring which part of an assembly line a part is currently traversing, but is not accurate enough to enable precise tooling or positioning. Figure 1.2 illustrates a part of the assembly line where tooling is done.

Many filtering methods have been explored to improve UWB tracking. For example, methods have been explored to improve the calculation of time of flight (TOF) using match filtering and a peak search technique [24]. A least square technique has also been used iteratively to improve accuracy by transforming a three-dimensional localization problem into a one-dimensional problem [33]. Bayesian filters have been used to track time of arrival (TOA) biases created by non line of sight (NLOS) conditions [10]. A particle filter augmented with a measurement noise map has also been used to improve tracking accuracy [30]. A particle filter has also been used with a model for sensor set noise [4].

In this work, we are using a map of an assembly line to constrain the motion tracking. This is similar to how a road map can be used to constrain position tracking for a GPS sensor. The idea is that the raw sensor measurements are constrained by

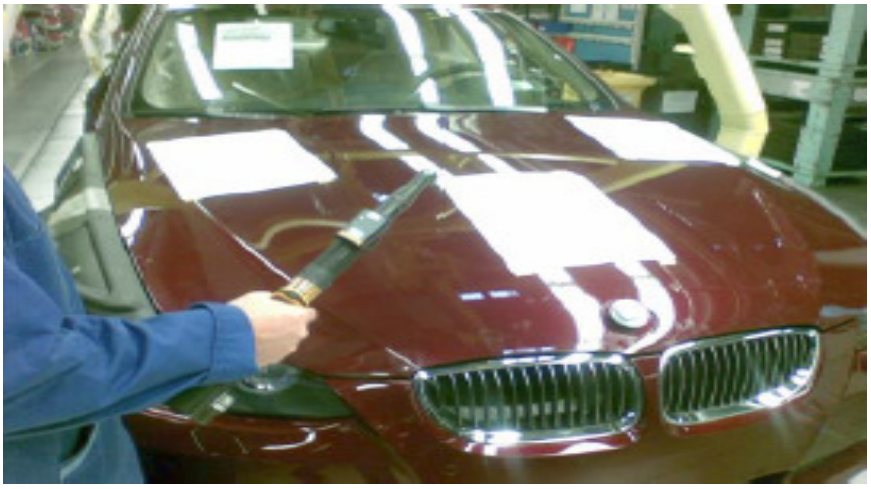

Figure 1.2: A station in the assembly line where tooling is done.

the a priori known map of motion along the assembly line. The following sections give background on global and local positioning systems, UWB indoor tracking and filtering.

1.1 Global and Local Positioning Systems

The Global Positioning System (GPS) was developed by the U.S Department of Defense (DoD) in the 1970s. It is an active global navigation satellite system (GNSS), which is a system of satellites providing geo-spatial tracking information. A GNSS calculates the distance or range of a transmitter by first computing the time taken for the radio frequency signal to propagate from the transmitter to the receiver and then multiplying that with the speed of light. Since the time taken for the signal can be the same for any place on a sphere around the transmitter, several such transmitters are used. The point of intersection of their spheres gives the position of the receiver. This process is called trilateration if 3 measurements are used; the general term is called multilateration. It is illustrated in 2D in figure 1.3. There are

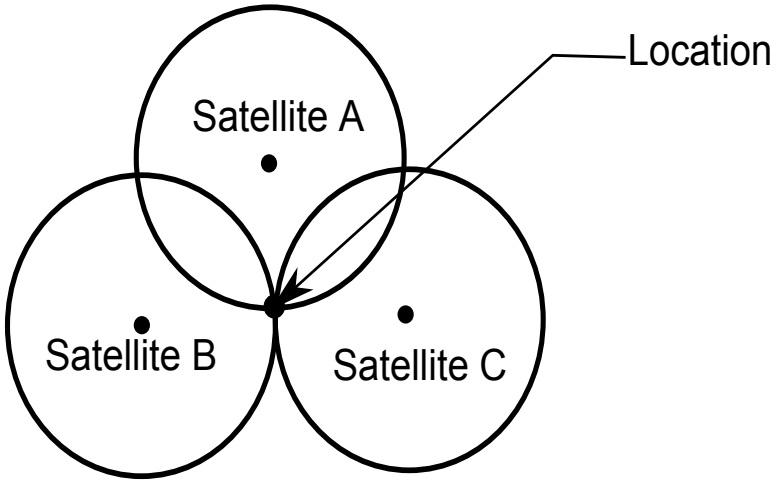

Figure 1.3: Trilateration.

several methods in which the range can be calculated but the basic principle remains the same. These include measuring angle of arrival (AOA), time of arrival (TOA) and time difference of arrival (TDOA).

A local positioning system (LPS) works on a principle similar to a GNSS. Here the tracking area is a lot smaller and is intended to work inside buildings. The GNSSs do not transmit signals with enough power to penetrate inside buildings. Hence a LPS is used in these areas. Unlike the GNSSs, one of the main requirements of a LPS signal is that it has to be capable of penetrating through walls, furniture and other things present inside buildings. Also, the accuracy should not get affected because of the clutter. The installation of such a system is one of the biggest challenges since the sensors must be mounted in such a way that there is good coverage of the area, cables need to be routed taking security into consideration and the placement and calibration of the sensors must be done accurately.

1.2 Ultra-wideband tracking

The Defense Advanced Research Projects Agency's (DARPA) in its report on the assessment of short-pulse wave technology introduced the term UWB to distinguish it from other conventional radar technologies [14]. UWB signalling was permitted for usage by the United States Federal Communication Commision in 2002 [8]. UWB signals are defined as signals with ultra short pulses ($<$ 1ns) with a low duty cycle ($<$ 0.5 %) capable of transmitting signals over a wide range of frequencies (3.1 to 10.6GHz simultaneously) and having a large bandwidth ($>$ 500 MHZ) [23]. Figure 1.4 shows the FCC approved frequency range for UWB signals [16]. UWB is being used for a variety of applications like for high bandwidth video and data transmission [11, 12, 27], radar for through wall imaging to detect people and objects [1, 6, 22, 26], medical imaging [5, 7, 9] and localization for inventory and target tracking [2, 13, 29, 34]. Our work makes use of an UWB system. Like the working of the GNSS, the UWB system estimates the range by multiplying the time of flight with the speed of light. The advantage of this system are the ease of installation, handling non line of sight (NLOS) and potential accuracy in tracking targets [12].

The main sources of noise present in the indoor tracking system are NLOS, multipath, synchronization, antenna effects, peak detection and sensor placement [31]. NLOS causes increased time of flight (TOF) hence directly affecting the range measurement. Multipath can also cause increased TOF measurement, especially if the direct path is attenuated. Since the UWB system calculates the range using TOA or TDOA, synchronization is very important as accurate clock references are needed. Accurate peak detection also affects TOA and TDOA measurements. Sensor placement can also affect the performance due to dilution of precision. Filters can be used to overcome some of these noise sources. The concept of filtering is explained in the

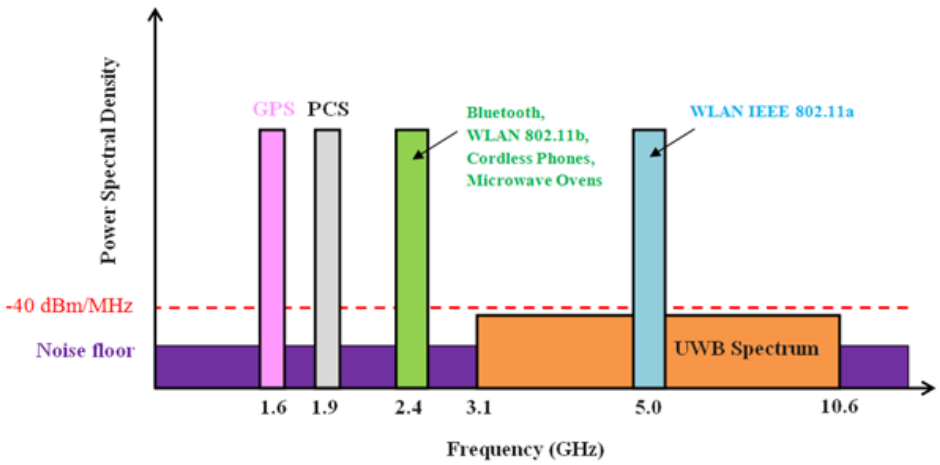

Figure 1.4: Frequency range of UWB spectrum.

next section.

1.3 Filtering

This section provides background on the technique of filtering. A filter iteratively updates the fit of a model. A model refers to a mathematical equation that can best describe the general shape or pattern of a particular set of data. Fit refers to finding the best set of parameters for a given set of data. The best set of parameters are the values of the unknown variables in the model that best fit the general shape of the given data. The filter can be used to estimate the past, present and future states of a system [32]. The following sections describe the components of filtering and two filtering techniques used in tracking applications.

1.3.1 State Variables

The state variables are the quantities that describe the behavior of the thing being tracked. When an object moving on an assemble line has to be tracked, one

can for example keep track of its position and velocity along the x and y directions. These can be represented as a vector.

$$X_t = \begin{bmatrix} x_t \\ \dot{x}_t \\ y_t \\ \dot{y}_t \end{bmatrix} \tag{1.1}$$

where x_t and y_t are the positions and $\dot{x}_t$ and $\dot{y}_t$ are the velocities in x and y direction at time t.

1.3.2 State Transition Equations

The state transition equations are a set of equations that describe the expected behavior of the the thing being tracked over a period of time. The state transition equations can be written to describe any desired model. For example, for the 2D state variables just described, the state transition equations could be written as

$$f = \begin{bmatrix} x_{t+1} = x_t + \dot{x}_t \delta t \\ \dot{x}_{t+1} = \dot{x}_t + a_{x,t} \\ y_{t+1} = y_t + \dot{y}_t \delta t \\ \dot{y}_{t+1} = \dot{y}_t + a_{y,t} \end{bmatrix} \tag{1.2}$$

where δt is the time period between two measurements. $a_{x,t}$ and $a_{y,t}$ are the dynamic noise in x and y at the time instance t. These equations assume that the thing is moving with a constant velocity.

The state transition equations can also be represented in matrix form as shown

in equation (1.3) to (1.5).

$$f = \left[x_{t+1} = \Phi x_t + A_t \right] \tag{1.3}$$

$$\Phi = \begin{bmatrix} 1 & \delta_t & 0 & 0 \\ 0 & 1 & 0 & 0 \\ 0 & 0 & 1 & \delta_t \\ 0 & 0 & 0 & 1 \end{bmatrix} \tag{1.4}$$

$$A_t = \begin{bmatrix} 0 \\ a_{x,t} \\ 0 \\ a_{y,t} \end{bmatrix} \tag{1.5}$$

where Φ is the state transition matrix and A_t is the dynamic noise.

1.3.3 Dynamic Noise

Dynamic noise refers to the uncertainty in predictions in the state transition equation. For example the value of $a_{x,t}$ and $a_{y,t}$ can be obtained from the distribution $N(0, \sigma_a^2)$. $N(0, \sigma_a^2)$ denotes a random, normally distributed variable with a mean of zero and a standard deviation of σ_a. The value of σ_a defines how large of an acceleration can be expected during each prediction interval. The dynamic noise covariance matrix Q represents the covariance of the set of dynamic noises. In the dynamic noise covariance matrix the zeros signify that there is no correlation between x and y axes. The discrete dynamic noise covariance matrix Q_t represents the covariance for a time

interval δ_t [20, 4].

$$Q_t = \begin{bmatrix} \delta_t^3/3 & \delta_t^2/2 & 0 & 0 \\ \delta_t^2/2 & \delta_t & 0 & 0 \\ 0 & 0 & \delta_t^3/3 & \delta_t^2/2 \\ 0 & 0 & \delta_t^2/2 & \delta_t \end{bmatrix} Q \tag{1.6}$$

$$Q = \begin{bmatrix} \sigma_{dx}^2 & 0 & 0 & 0 \\ 0 & \sigma_{dx}^2 & 0 & 0 \\ 0 & 0 & \sigma_{dy}^2 & 0 \\ 0 & 0 & 0 & \sigma_{dy}^2 \end{bmatrix} \tag{1.7}$$

1.3.4 Observation equation

The observation equations are a set of equations that describe the expected range of measurements given the current state of the thing being tracked. The observation is obtained from the sensor. These give the position of the thing being tracked. Measurement noise is part of the observation equation and is used to describe the potential corruption of the observations. The observed values at any time can be represented as

$$Y = \begin{bmatrix} \hat{x_t} \\ \hat{y_t} \end{bmatrix} \tag{1.8}$$

where $\hat{x_t}$ and $\hat{y_t}$ are the measurements from the sensor. The observation equation can be represented as

$$g = \begin{bmatrix} \hat{x_t} = x_t + v_{x,t} \\ \hat{y_t} = y_t + v_{y,t} \end{bmatrix} \tag{1.9}$$

where $v_{x,t}$ and $v_{y,t}$ represent the measurement noise. The observation equations can also be represented in matrix form as

$$g = \left[Y_t = MX_t + N_t \right] \tag{1.10}$$

where the observation matrix M is given by

$$M = \begin{bmatrix} 1 & 0 & 0 & 0 \\ 0 & 0 & 1 & 0 \end{bmatrix} \tag{1.11}$$

and the observation noise matrix is written as

$$N = \begin{bmatrix} v_{x,t} \\ v_{y,t} \end{bmatrix} \tag{1.12}$$

1.3.5 Measurement Noise

The measurement noise is the uncertainty in the sensor readings. The measurement noise covariance matrix is show in (1.13). σ_x^2 and σ_y^2 represent the variances and $\sigma_{x,y}$ is the covariance along the X and Y axes respectively.

$$R = \begin{bmatrix} \sigma_x^2 & \sigma_{x,y} \\ \sigma_{x,y} & \sigma_y^2 \end{bmatrix} \tag{1.13}$$

1.3.6 Kalman Filter

A Kalman filter is an algorithm which uses a series of measurements observed over time, assumed to contain measurement noise, and produces estimates of unknown variables. The variables are the state variable of interest. The noise arises from the

sensor which is used to measure the variable. Inaccuracies arise from the predictions of the system due to dynamic noise. The Kalman filter is explained here with reference to tracking a thing in a two dimensional space.

The algorithm works in a two-step process: in the prediction step, the Kalman filter produces estimates of the current state variables, along with their uncertainties [17]. Once the outcome of the next measurement is observed, these estimates are updated using a weighted average, with more weight being given to estimates with higher certainty.

The first step in the Kalman filter is to predict the next state

$$X_{t,t-1} = \Phi X_{t-1,t-1} \tag{1.14}$$

Once the state is predicted, the next state covariance matrix is also predicted

$$S_{t,t-1} = \Phi S_{t-1,t-1} \Phi^T + Q \tag{1.15}$$

Measurements are then obtained from the sensor

$$Y_t = \begin{bmatrix} \hat{x_t} \\ \\ \hat{y_t} \end{bmatrix} \tag{1.16}$$

After the measurement is obtained, the innovation is calculated as the difference between the estimated measurement and the actual measurement.

$$J = Y_t - M X_{t,t-1} \tag{1.17}$$

Next, the covariance of innovation is calculated.

$$\mathrm{COV}(J) = MS_{t,t-1}M^T + R \tag{1.18}$$

From the covariance of innovation obtained in the last step, the gain matrix is calculated as

$$K_t = S_{t,t-1}M^T\mathrm{COV}(J)^{-1} \tag{1.19}$$

Using the Kalman gain, the state covariance matrix is updated.

$$S_{t,t} = [I - K_tM]S_{t,t-1} \tag{1.20}$$

Finally the updated state is calculated as

$$X_{t,t} = X_{t,t-1} + K_tJ \tag{1.21}$$

These steps form the main loop of the filter.

The Kalman filter can only be used if the state transition and the observation equations are linear and the measurement noise is normally distributed. The extended Kalman filter (EKF) can be used for non linear state transition equations. The EKF calculates Jacobians at each time instant to linearize the problem [32]. The Kalman filter and the EKF break down when the observation distribution is not Gaussian.

1.3.7 Particle Filtering

The Kalman filter assumes that the state transition and observation equations are linear and that all noises are Gaussian. Our experiments use equations that have non-linearities and non-Gaussian noises. We therefore use the particle filter.

A particle filter is a sequential Monte Carlo method used for estimating non-Gaussian distributions [17]. Monte Carlo methods are a class of computational algorithms that rely on repeated random sampling to compute their results. The samples from the Monte Carlo method in a particle filter are called particles. The particles with corresponding weights are used to form an approximation of a probability density function. Importance sampling is performed on the probability density function. Importance sampling is a general technique for estimating properties of a particular distribution. The basic methodology in importance sampling is to choose a distribution which encourages the important values. The important values, in this case particles, are given higher weights and the desired output is computed from the mean.

1.3.8 Particle filter algorithm

The particle filter uses a Monte Carlo approximation. The distribution $p(x|y)$ is represented using a number of samples. In this context of the particle filter, the samples are called particles. They are denoted as:

$$\chi = \{x^{(m)}, w^{(m)}\}_{m=1}^{M} \tag{1.22}$$

The number of state spaces or samples used for our experiment is $M = 1000$. The state of each of the particles can be initialized with the first measurement or with zeros. The weight of each particles is initialized to $\frac{1}{M}$ in our experiment.

Like other filters, the particle filter algorithm follows a predict-update cycle. First, each particle m is propagated through the state transition equation:

$$\{x_t^{(m)} = f(x_{t-1}^{(m)}, a_t^{(m)})\}_{m=1}^{M} \tag{1.23}$$

The value $a_t^{(m)}$ represents the dynamic noise from $t-1$ to t, and is randomly and independently calculated for each particle m. The new measurement vector y_t is obtained and the weight of each of the particles are updated.

$$\tilde{w}_t^{(m)} = w_{t-1}^{(m)} \cdot p(y_t|x_t^{(m)}) \tag{1.24}$$

where

$$p(y_t|x_t^{(m)}) = exp(\frac{-(y^{(m)} - y)^2}{2\sigma_n^2}) \tag{1.25}$$

and

$$y^{(m)} = g(x^{(m)}, 0) \tag{1.26}$$

Once the weights are calculated, they are normalized to sum up to 1.

$$w_t^{(m)} = \frac{\tilde{w}_t^{(m)}}{\sum_{m=1}^{M} \tilde{w}_t^{(m)}} \tag{1.27}$$

The desired output is then obtained as the mean of the particles.

$$E[x_t] \approx \sum_{m=1}^{M} x_t^{(m)} \cdot w_t^{(m)} \tag{1.28}$$

After a few transitions there is a possibility that most of the particles have very low weights. This results in very few particles contributing to the approximation of the probability distribution function. Hence there is a check to see if resampling is necessary to remove these particles with low probability. More copies of particles with higher probability are added to better approximate the probability distribution function. A number of resampling methods can be used for this purpose [28], *select with replacement* is used in our experiments [3].

To check whether resampling is necessary, the coefficient of variation (CV) and effective sample size (ESS) are computed.

$$CV = VAR\frac{(w^{(m)})}{E^2[w^{(m)}]} = \frac{1}{M}\sum_{m=1}^{M}(M \cdot w^{(m)} - 1)^2 \tag{1.29}$$

$$ESS = \frac{M}{1 + CV} \tag{1.30}$$

The effective sample size describes how many particles have an appreciable weight. If ESS is less than 0.5 M (threshold is set to 50% of the particles) resampling is done in our experiment.

These steps form the main loop of the filter. The particle filter can be used for problems with linear and non-linear state transition and observation equations as well as any dynamic and noise distributions.

1.4 Novelty

In this thesis, we use a map of an assembly line to improve UWB position tracking. This is similar to how a road map can be used to improve position tracking for an automobile using a GPS [15, 21]. The essence of the idea is that position measurements are constrained to locations on the path (road or assembly line). For our problem we use an UWB indoor tracking system. Other types of maps have been used to improve UWB position tracking. For example, a map of environment noise has been shown to improve position tracking by up to 15% [30]. Floorplan maps have been used to constrain motion tracking from traversing through walls [25]. To our knowledge, this is the first time that a map of an assembly line has been used to improve UWB position tracking.

Chapter 2

Research Design and Methods

2.1 Introduction

We model an assembly line using a piece-wise function of linear segments. Each segment extends from a starting position x_a, y_a to an ending position x_b, y_b. We assume that the target moving along the assembly line takes some unknown time to travel between these points, depending on the velocity at which it moves. We also assume that the object can speed up, slow down, or even stop while moving along a segment.

Figure 2.1 shows three example segments. The first and third segments show motion in x and y, the second segment is a pause at the joining point of the first and third segments. Specifically, segment one can be modeled as $(x_A, y_A), (x_B, y_B)$, segment two as (x_B, y_B), (x_B, y_B) and segment three as $(x_B, y_B), (x_C, y_C)$.

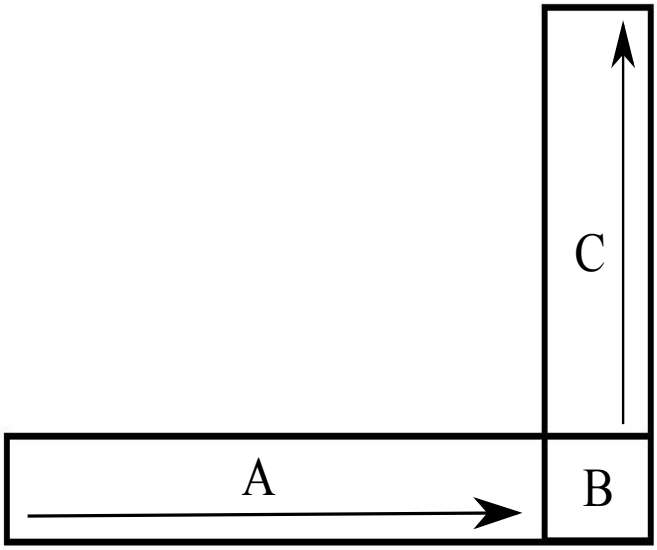

Figure 2.1: Example segments modeling an assembly line.

2.2 Filter design

This section describes the particle filter design which we use for our experiment. We use the particle filter because our state transition equation (equation 2.2) and observation equation (equation 2.5) are nonlinear. The dynamic noise is also not purely Gaussian.

We model the motion along the assembly line using a dummy variable d that tracks the distance along the path. Formally, our state X_t is defined as:

$$X_t = \begin{bmatrix} d_t \\ \dot{d}_t \end{bmatrix} \tag{2.1}$$

where d_t represents a position, and $\dot{d}_t$ represents the velocity.

Our state transition equation f is modelled as

$$f(x_t, a_t) = \begin{bmatrix} d_{t+1} = d_t + \dot{d}_t T \\ \dot{d}_{t+1} = max(0, \dot{d}_t + a_t) \end{bmatrix} \tag{2.2}$$

where a_t represents random changes in velocity (accelerations or decelerations) at time t. We model a_t using $N(0, \sigma_a)$, a zero-mean normal distribution with σ_a defining the standard deviation of the expected random change in velocity. We use the max operator to enforce the constraint that the velocity can speed up or slow down but cannot reverse; in other words, the target being tracked may pause while moving along a segment, but it cannot back up.

Our observations Y_t are obtained from an UWB tracking system:

$$\hat{Y_t} = \begin{bmatrix} \hat{x_t} \\ \hat{y_t} \end{bmatrix} \tag{2.3}$$

The measurements can take any values in the x, y space.

The filter estimate is mapped to the corresponding point on the x, y space. This is done for us to calculate the weight of the particles which requires the probability distribution used in equation 1.25 on section 1.3.7. Figure 2.2 illustrates this mapping.

$$Y_t = \begin{bmatrix} x_t \\ y_t \end{bmatrix} \leftarrow \begin{bmatrix} d_t \end{bmatrix} \tag{2.4}$$

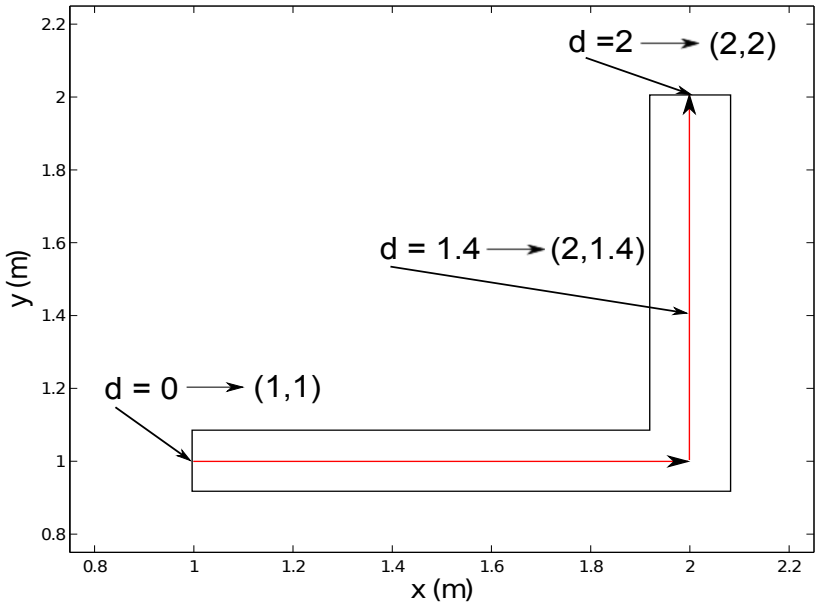

Figure 2.2: Mapping of d to (x,y). The red line with arrows shows the path taken.

2.3 Ubisense system

We use an UWB positioning system manufactured by the U.K. based company Ubisense, Inc. The Ubisense tags transmit the UWB pulses which are detected by 8 sensors mounted in the Riggs facility. Figure 2.3 shows the Ubisense tag and sensor. The system estimates the range using angle of arrival (AOA) and time differene of arrival (TDOA) techniques with as few as two sensors required for a position estimate [18, 19].

2.4 Facility

The experiment was carried out in our facility in the basement of Riggs Hall at Clemson University. The UWB tracking area is approximately 8m x 9m which covers

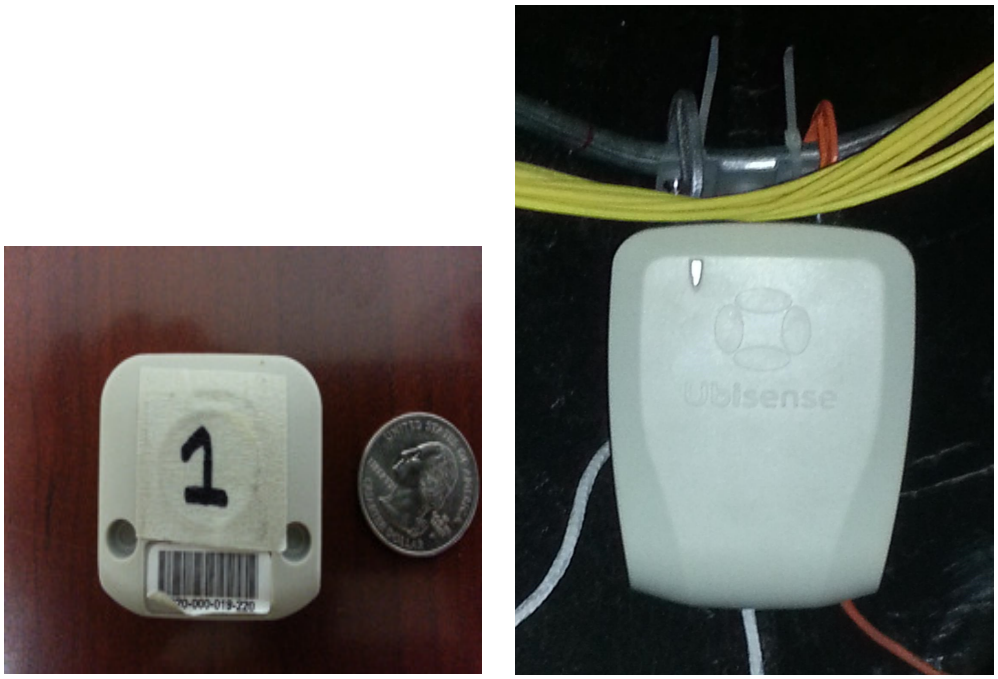

Figure 2.3: (a) UWB tag which is placed on the object to be tracked. (b) UWB sensor that is mounted in the facility.

the majority of the laboratory and a part of the adjacent hallway. The path for our experiment was completely inside the laboratory. Figure 2.4 shows a picture of the laboratory. The laboratory is separated with the hallway by a 20cm thick concrete wall. The walls in the facility are 5m high with false ceilings at a height of 3m. The false ceiling are made up of thermocol and placed on metal railings. Two cupboards are present inside the laboratory. Eight Ubisense sensors are mounted in this facility with five inside the laboratory and three in the adjacent hallway.

2.5 Data collection

Data was collected using the cart shown in Figure 2.5. The tag of the UWB system is mounted on the cart at a height of 78cm from the ground. The cart is equipped with a laser mounted below the tag (pointing down) which helps in following

Figure 2.4: Laboratory where the data collection was carried out.

the path. Three different types of motion are followed along the path, these are called the three situations. In the first situation, a constant velocity is maintained. In the second situation, a constant velocity is maintained for the motion but there are halts for a fixed period of time at the segment ends. The third situation has no halts, but the velocity of motion along the segments differ. The Ubisense system provides raw measurements of the data along the X and Y axes. Three sets of recordings are collected for each of the situations.

The path followed for our experiment is illustrated in Figure 2.6. The starting position and the ending position of the segments of the path are listed in Table 2.1. The different segments of the path are labelled from A to E.

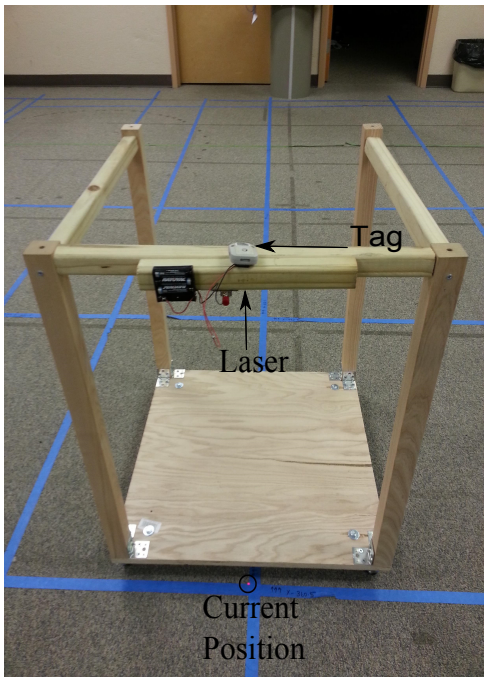

Figure 2.5: Cart used for data collection.

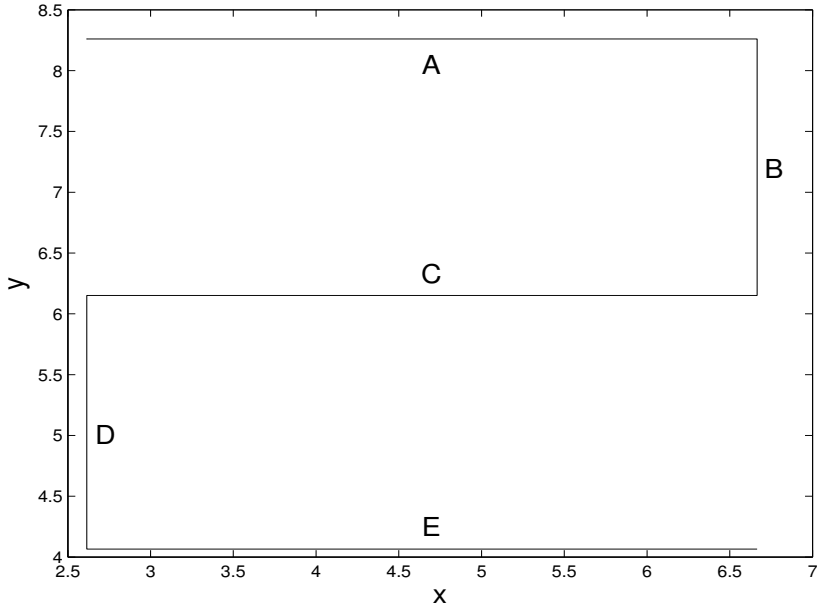

Figure 2.6: Path followed for data collection.

Table 2.1: End points of the segments of the path used for the experiment (in meters)

Segment	x_a	y_a	x_b	y_b	d
A	2.62	8.26	6.67	8.26	4.05
B	6.67	8.26	6.67	6.15	6.16
C	6.67	6.15	2.62	6.15	10.21
D	2.62	6.15	2.62	4.07	12.29
E	2.62	4.07	6.67	4.07	16.34

The mapping in equation 2.4 can be written for our path as

$$Y_t = \begin{bmatrix} x_t = d_t + 2.615 & \text{if } 0 \leq d_t \leq 4.05 \\ y_t = 8.26 & \\ x_t = 6.665 & \text{if } 4.05 < d_t \leq 6.159 \\ y_t = 8.26 - d_t + 4.05 & \\ x_t = 6.665 - d_t + 6.159 & \text{if } 6.159 \leq d_t \leq 10.209 \\ y_t = 6.151 & \\ x_t = 2.615 & \text{if } 10.209 \leq d_t \leq 12.295 \\ y_t = 6.151 - d_t + 10.209 & \\ x_t = 2.615 + d_t + 12.295 & \text{if } d_t > 12.295 \\ y_t = 4.065 & \end{bmatrix} \tag{2.5}$$

Figure 2.7 shows one set of data collected from each of the three situations. The plot of raw data and ground truth for the three situations are shown on the left side and their respective velocity profiles are indicated to their right. The process to obtain ground truth data is explained in section 2.6.

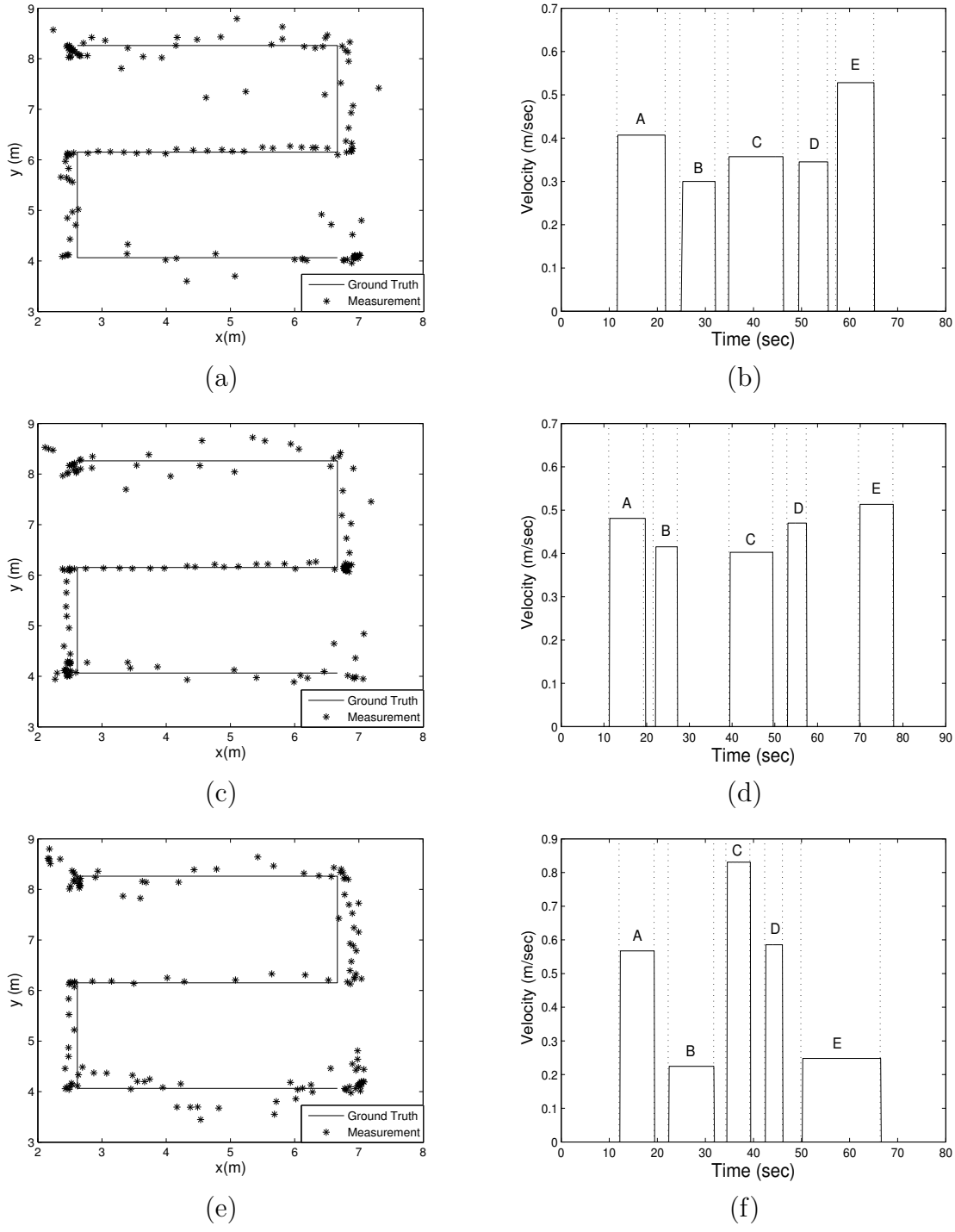

Figure 2.7: (a) Plot of raw measurement and ground truth for situation 1,2 and 3 are shown on (a),(c) and (e) respectively. (b) Velocity of the cart when travelling on the different segments for the measurement obtained in (a), (c) and (e) are shown on (b), (d) and (f) respectively.

2.6 Ground truth

Since the path is fixed, the start location and end location are known. The position with respect to time needs to be calculated for points between the ends. In order to do that, the time interval of motion and velocity in each of the segments are calculated. The least square method is used to calculate the time. The cart is initially placed in the start position and measurements are collected for 10 seconds at this position before starting to move. When the end of the path is reached, there is a wait of another 10 seconds before ending the recording. This gives flat regions in the starting and ending and linear regions and flat regions in between. A subset of measurements are selected in each region (linear and flat) and are used to provide a least square fit to the set of measurements in that region. The measurement that lies closest to the intersection of these points gives the start, end or change in dynamics. Since motion can be either in x or y, the direction of motion is used to calculate the time.

For example, in the path on figure 2.6, motion is in x in the first segment. Then the time of start and the end of motion are obtained from the plot of x with time. Figure 2.8(a) illustrates this approach. Let the motion start time and end time obtained be t_1 and t_2. At the end of segment A there might be rest for a period of time or motion could continue. Motion would be along segment B in y-direction. The motion start time and end time are obtained from the y versus time plot, Figure 2.8(b). Let these times be t_3 and t_4. In the interval of time between t_2 and t_3, position is at the end of segment A.

Now that the start time and end time of travelling in the segments, as well as the start and end points of the segments are known, the velocity travelled in each of the segments are calculated. Multiplying the velocity with the time at which the

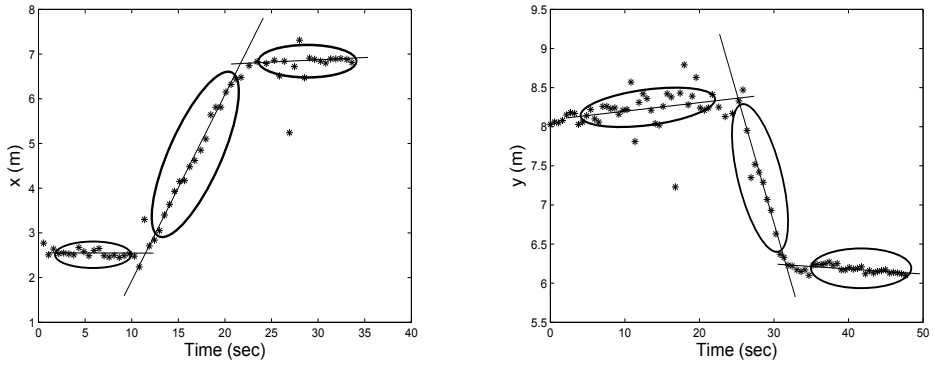

(a) (b)

Figure 2.8: Least square method to obtain the ground truth using x and y coordinates shown in (a) and (b) respectively.

measurement was obtained the corresponding ground truth position of the tag at that instant is known. For segment A, where the motion is in x-direction the x ground truth can be calculated as

$$\check{x_t} = \frac{D_A}{T} \times t \tag{2.6}$$

where D_A is the length of segment A and T is the time taken to traverse the path (from our earlier example t_2 - t_1) and $\check{x}$ are the ground truth at time instant t. The y ground truth ($\check{y}$) for segment A will be constant(equal to the y coordinate of the start point of segment A).

On the other hand for segment B the value of $\check{x}$ will be a constant(equal to the x coordinate of the start point of segment A) and the $\check{y}$ can be calculated in a similar way as $\check{x}$ for segment A. For the other segments too, the ground truth is calculated in a similar way.

$$\check{y_t} = \frac{D_B}{T} \times t \tag{2.7}$$

2.7 Error Metric

To evaluate the performance of our filter we define an error metric. The average distance between the filtered data and the corresponding ground truth data is calculated over the total number of measurements. This distance is known as the root mean square error(RMSE) or deviation and can be defined as

$$RMSE = \sqrt{\frac{1}{N}\sum_{i=1}^{N}(\check{x}_i - x_i)^2 + (\check{y}_i - y_i)^2} \tag{2.8}$$

where $\check{x}_i$ and $\check{y}_i$ represent the ground truth position and x_i and y_i represents the filter output for the measurement i. N is the total number of measurements.

Chapter 3

Results

The value of measurement noise was calculated as the average error in the measurements using all the data sets. Dynamic noise for the Kalman filter as well as the particle filter were set by varying the dynamic noise over a range of 0 to 100 cm and then finding the value of the dynamic noise for the minimum error. This too was calculated using all the data sets. Once the value of measurement noise and dynamic noise were calculated they were fixed for all subsequent experiments. Figures 3.1 to 3.6 show the results for one trial for each of the three situations tested. The filter output as well as the errors are shown. In these figures the particle filter output always stays on the assembly line while the Kalman filter strays away. The error of the particle filter is hard to make out in the figure of the assembly line. The error comparison figures gives us a much better idea of the performance, the average error is also indicated on them with dashed lines. It is evident that the particle filter error is below the Kalman filter error for a large part of the tracking period.

The particle filter uses a Monte Carlo approach so a single trial does not necessarily provide a representative output. Ten iterations were done for each of the data sets and average error was computed and is shown in table 3.1. The average

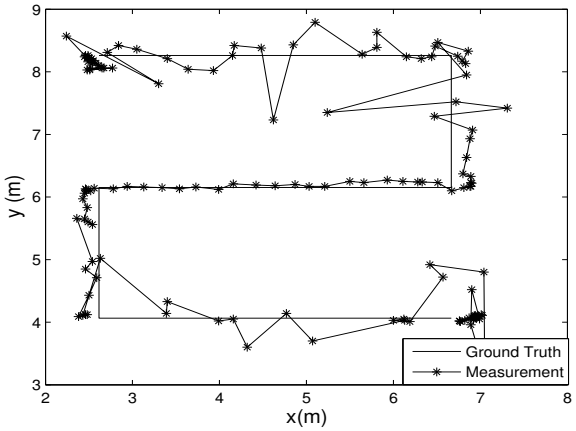

(a)

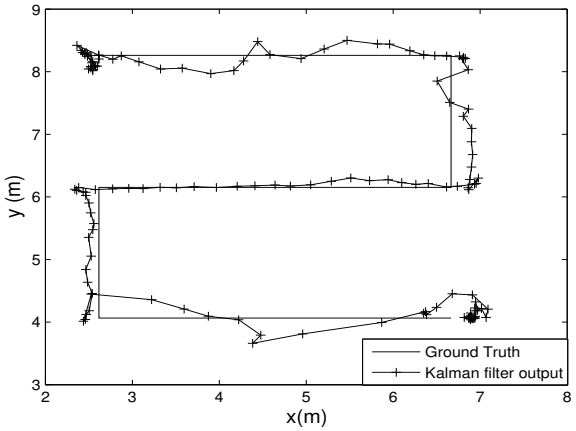

(b)

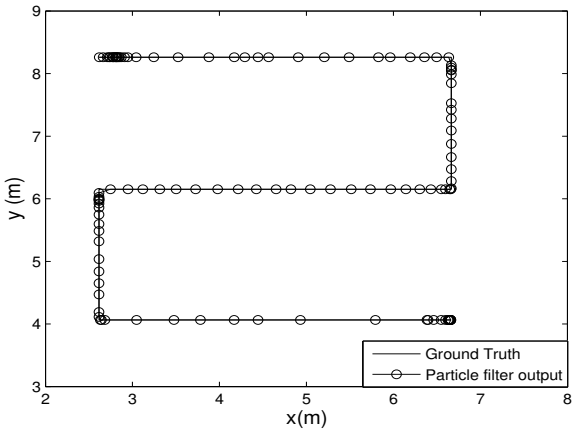

(c)

Figure 3.1: Plot of the raw measurement and the filter outputs for situation 1.

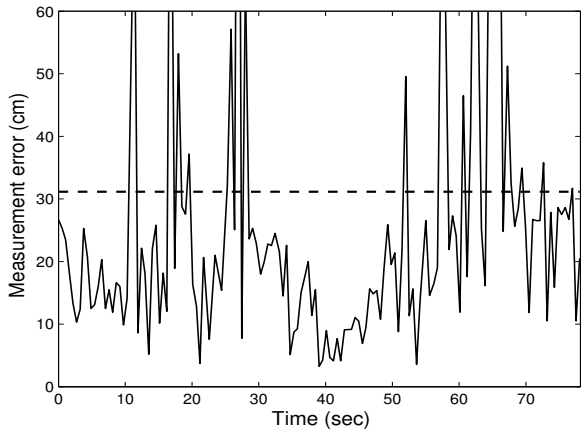

(a)

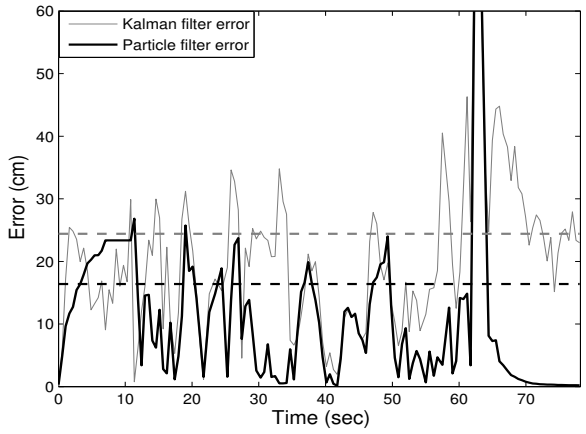

(b)

Figure 3.2: Error plots for situation 1 (a) Shows the measurement error. Average measurement error is 31.1 cm. (b) Shows the error of the particle filter compared to the Kalman filter with an average improvement of 8.1 cm.

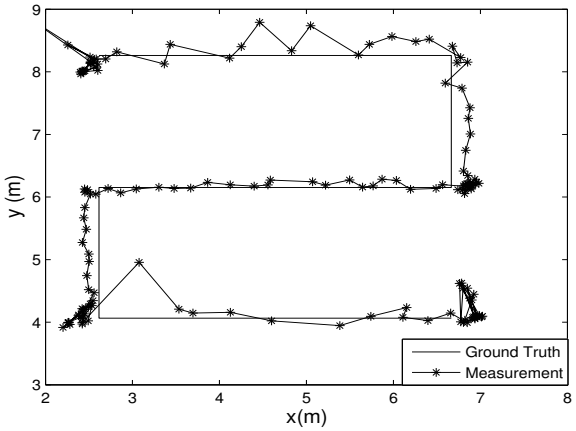

(a)

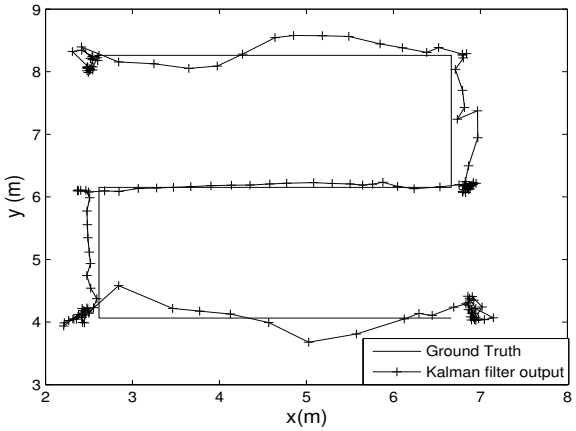

(b)

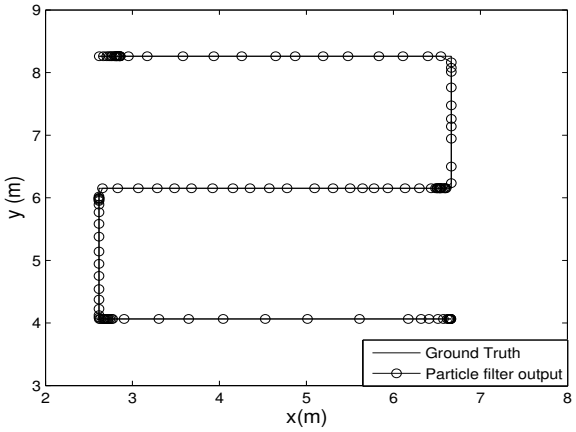

(c)

Figure 3.3: Plot of the raw measurement and the filter outputs for situation 2.

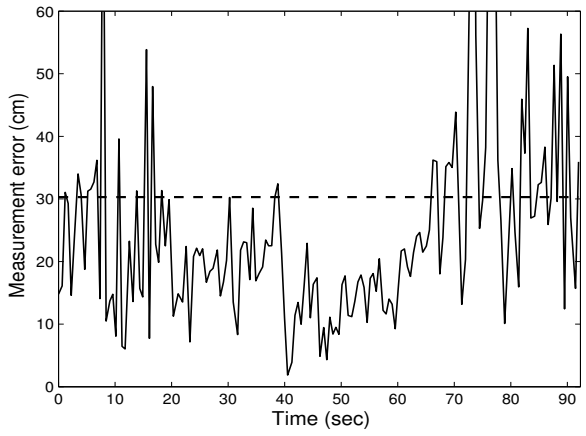

(a)

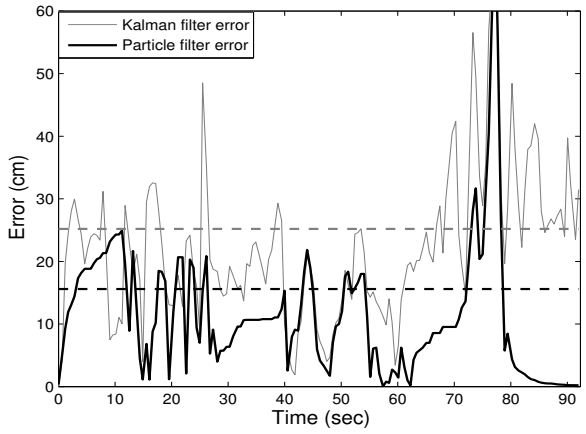

(b)

Figure 3.4: Error plots for situation 2 (a) Shows the measurement error. Average measurement error is 30.3 cm. (b) Shows the error of the particle filter compared to the Kalman filter with an average improvement of 9.6 cm.

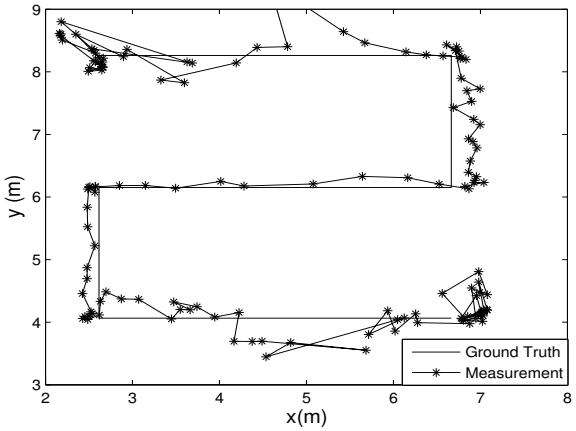

(a)

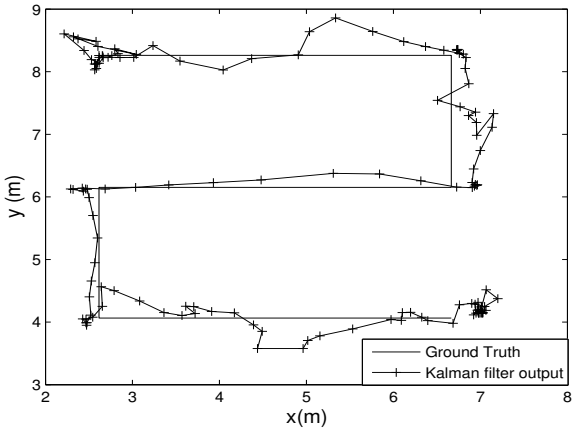

(b)

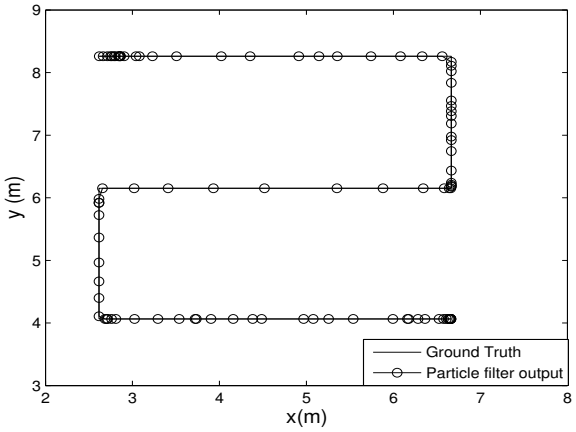

(c)

Figure 3.5: Plot of the raw measurement and the filter outputs for situation 3.

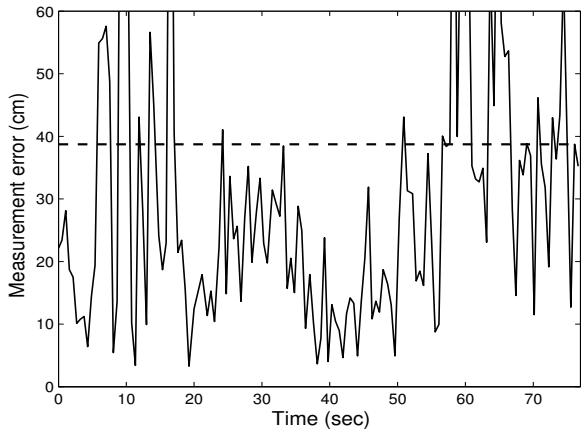

(a)

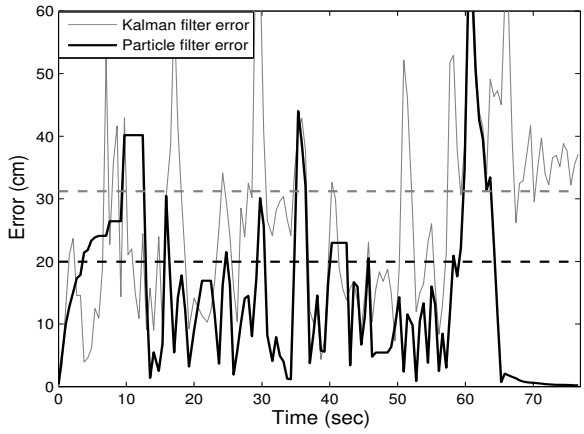

(b)

Figure 3.6: Error plots for situation 3 (a) Shows the measurement error. Average measurement error is 38.7 cm. (b) Shows the error of the particle filter compared to the Kalman filter with an average improvement of 11.3 cm.

error of the particle filter for all the data sets is 17.6 cm while that for the Kalman filter is 27.9 cm. The particle filter gives a 55% improvement in the estimation of the position compared to the measurements and a 37% improvement when compared to the Kalman filter.

Table 3.1: Error comparison of the filter outputs (in cm).

Situation	Data Set	Measurement	Kalman	Particle
Situation 1	Set 1	31.1	24.4	16.3
	Set 2	31.2	25.8	16.9
	Set 3	52.8	31.7	16.1
Situation 2	Set 1	30.3	25.2	15.8
	Set 2	33.5	24.3	14.9
	Set 3	29.4	24.5	13.7
Situation 3	Set 1	38.7	31.2	20.2
	Set 2	44.8	31.1	19.6
	Set 3	60.8	33.7	24.8
Average error		39.2	27.9	17.6

Chapter 4

Conclusion and Future work

In this thesis we have designed a filter for tracking objects on an assembly line using an ultra wide-band positioning system. We designed a particle filter because the state transition equations were not linear and the dynamic noise was not purely Gaussian. Our filter has reduced the tracking error from 39.2 cm to 17.6 cm, improvement of 55%. The result is also better when compared with a 2D Kalman filter which has a tracking error of 27.9 cm, improvement of 37%. This reduction in tracking error could help promote the use of an UWB system as a central tracking system in an assembly line, thereby replacing other sensors like proximity and RFID required to keep a track of the things moving on the assembly line. The tracking can also be used for tooling by using the position estimates from the UWB in the factory control system.

The filter presented in this thesis could be extended to include a segment ID as a state variable. This would require including it in the state transition and observation equations. The benefit would be seen during periods of rest at segment joins. The filter presented in this thesis tends to overshoot such rest periods because it assumes continuous motion. A filter incorporating a segment ID for a state variable

could recognize the transition at a junction and change to a piecewise function that is pure rest.

Another possibility for future work is to extend the observation equation to detect events where a tracked object may leave an assembly line. This could be done by tracking the cumulative error between a standard Kalman filter and a map-constrained filter, identifying an event when they sufficiently diverge. This is similar to how an automobile GPS identifies when a car has gone off a given road.

Bibliography

[1] F. Ahmad, Y. Zhang, and M. Amin, "Three-dimensional wideband beamforming for imaging through a single wall," *IEEE Geoscience and Remote Sensing Letters,*, vol. 5, no. 2, pp. 176–179, 2008.

[2] N. Alsindi and K. Pahlavan, "Cooperative localization bounds for indoor ultra-wideband wireless sensor networks," *EURASIP Journal on Advances in Signal Processing*, vol. 2008, p. 125, 2008.

[3] M. Arulampalam, S. Maskell, N. Gordon, and T. Clapp, "A tutorial on particle filters for online nonlinear/non-gaussian bayesian tracking," *IEEE Transactions on Signal Processing,*, vol. 50, no. 2, pp. 174–188, 2002.

[4] S. Banerjee, "Improving accuracy in ultra-wideband indoor position tracking through noise modeling and augmentation," Ph.D. dissertation, Clemson University, 2012.

[5] C. Bilich, "Bio-medical sensing using ultra wideband communications and radar technology: A feasibility study," in *Pervasive Health Conference and Workshops, 2006.* IEEE, 2006, pp. 1–9.

[6] R. Chandra, A. Gaikwad, D. Singh, and M. Nigam, "An approach to remove the clutter and detect the target for ultra-wideband through-wall imaging," *Journal of Geophysics and Engineering*, vol. 5, no. 4, p. 412, 2008.

[7] X. Chen, J. Liang, S. Wang, Z. Wang, and C. Parini, "Small ultra wideband antennas for medical imaging," in *Antennas and Propagation Conference, 2008. LAPC 2008. Loughborough.* IEEE, 2008, pp. 28–31.

[8] F. C. Commission *et al.*, "Revision of part 15 of the commissions rules regarding ultra-wideband transmission systems. first report and order, et docket 98-153, fcc 02-48; adopted: February 14, 2002; released: April 22, 2002," 2002.

[9] S. Davis, B. Van Veen, S. Hagness, and F. Kelcz, "Breast tumor characterization based on ultrawideband microwave backscatter," *IEEE Transactions on Biomedical Engineering,*, vol. 55, no. 1, pp. 237–246, 2008.

[10] B. Denis, L. Ouvry, B. Uguen, and F. Tchoffo-Talom, "Advanced bayesian filtering techniques for uwb tracking systems in indoor environments," in *2005 IEEE International Conference on Ultra-Wideband, 2005. ICU 2005.* IEEE, 2005, pp. 6–pp.

[11] A. Dmitriev, B. Kyarginskii, A. Panas, D. Puzikov, and S. Starkov, "Ultrawideband direct chaotic data transmission in the microwave range," *Technical Physics Letters*, vol. 29, no. 1, pp. 72–74, 2003.

[12] R. Fontana, "Recent system applications of short-pulse ultra-wideband (uwb) technology," *IEEE Transactions on Microwave Theory and Techniques,*, vol. 52, no. 9, pp. 2087–2104, 2004.

[13] R. Fontana and S. Gunderson, "Ultra-wideband precision asset location system," in *IEEE Conference on Ultra Wideband Systems and Technologies, 2002. Digest of Papers. 2002.* IEEE, 2002, pp. 147–150.

[14] C. Fowler, J. Entzminger, J. Corum *et al.*, "Assessment of ultra-wideband(uwb) technology," *IEEE Aerospace and Electronic Systems Magazine*, vol. 5, no. 11, pp. 45–49, 1990.

[15] F. Gustafsson, F. Gunnarsson, N. Bergman, U. Forssell, J. Jansson, R. Karlsson, and P. Nordlund, "Particle filters for positioning, navigation, and tracking," *IEEE Transactions on Signal Processing,*, vol. 50, no. 2, pp. 425–437, 2002.

[16] O. Haraz. (2012, November) Why do we need ultra-wideband? [Online]. Available: http://www.vlsiegypt.com/home/?p=518

[17] A. Hoover, "Lecture notes - ece 854," 2012. [Online]. Available: http://www.ces.clemson.edu/~ahoover/ece854/

[18] U. Inc., "Location engine configuration user manual," 2008.

[19] U. Inc. (2012, May) Ubisense precise location. [Online]. Available: http://www.ubisense.net/en/resources/factsheets/ubisense-precise-location.html

[20] A. Kelly, "A 3d state space formulation of a navigation kalman filter for autonomous vehicles," DTIC Document, Tech. Rep., 1994.

[21] E. Krakiwsky, C. Harris, and R. Wong, "A kalman filter for integrating dead reckoning, map matching and gps positioning," in *IEEE PLANS'88., IEEE Position Location and Navigation Symposium, 1988. Record. Navigation into the 21st Century.* IEEE, 1988, pp. 39–46.

[22] C. Lai and R. Narayanan, "Through-wall imaging and characterization of human activity using ultrawideband (uwb) random noise radar," in *Defense and Security.* International Society for Optics and Photonics, 2005, pp. 186–195.

[23] H. Liu, H. Darabi, P. Banerjee, and J. Liu, "Survey of wireless indoor positioning techniques and systems," *IEEE Transactions on Systems, Man, and Cybernetics, Part C: Applications and Reviews,*, vol. 37, no. 6, pp. 1067–1080, November 2007.

[24] Z. Low, J. Cheong, C. Law, W. Ng, and Y. Lee, "Pulse detection algorithm for line-of-sight (los) uwb ranging applications," *IEEE Antennas and Wireless Propagation Letters,*, vol. 4, pp. 63–67, 2005.

[25] P. Meissner, C. Steiner, and K. Witrisal, "Uwb positioning with virtual anchors and floor plan information," in *7th Workshop on Positioning Navigation and Communication (WPNC), 2010*. IEEE, 2010, pp. 150–156.

[26] S. Nag, M. Barnes, T. Payment, and G. Holladay, "Ultrawideband through-wall radar for detecting the motion of people in real time," in *AeroSense 2002*. International Society for Optics and Photonics, 2002, pp. 48–57.

[27] D. Porcino and W. Hirt, "Ultra-wideband radio technology: potential and challenges ahead," *IEEE Communications Magazine,*, vol. 41, no. 7, pp. 66–74, 2003.

[28] I. Rekleitis, "A particle filter tutorial for mobile robot localization," *Centre for Intelligent Machines, McGill University*, vol. 3480, 2004.

[29] M. Soliman, T. Morimoto, and Z. Kawasaki, "Three-dimensional localization system for impulsive noise sources using ultra-wideband digital interferometer technique," *Journal of Electromagnetic Waves and Applications*, vol. 20, no. 4, pp. 515–530, 2006.

[30] W. Suski, "A study of environment noise in ultra-wideband indoor position tracking," Ph.D. dissertation, Clemson University, 2012.

[31] W. Suski, S. Banerjee, and A. Hoover, "System-level noise of an ultra-wideband tracking system," in *11th International Conference on Information Science, Signal Processing and their Applications (ISSPA), 2012*. IEEE, 2012, pp. 634–639.

[32] G. Welch and G. Bishop, "An introduction to the kalman filter," Department of Computer Science,University of North Carolina at Chapel Hill, Chapel Hill, North Carolina, Tech. Rep. TR 95-041, July 2006.

[33] J. Yan, C. Tiberius, P. Teunissen, G. Bellusci, and G. Janssen, "A framework for low complexity least-squares localization with high accuracy," *IEEE Transactions on Signal Processing,*, vol. 58, no. 9, pp. 4836–4847, 2010.

[34] D. Young, C. Keller, D. Bliss, and K. Forsythe, "Ultra-wideband (uwb) transmitter location using time difference of arrival (tdoa) techniques," in *Conference Record of the Thirty-Seventh Asilomar Conference on Signals, Systems and Computers, 2004.*, vol. 2. IEEE, 2003, pp. 1225–1229.